

Transport in integrable and perturbed easy-axis Heisenberg chain: Thouless approach

J. Pawłowski,¹ M. Mierzejewski,¹ and P. Prelovšek²

¹*Institute of Theoretical Physics, Faculty of Fundamental Problems of Technology,
Wrocław University of Science and Technology, 50-370 Wrocław, Poland*

²*Jožef Stefan Institute, SI-1000 Ljubljana, Slovenia*

We study transport in the spin chains by employing the Thouless approach based on the level sensitivity to the boundary conditions, R . Although spin transport in the integrable easy-axis XXZ model is diffusive, corresponding R is much closer to ballistic chains than to chaotic diffusive systems. In the case of the grand canonical ensemble this observation can be rigorously justified, while in the case of the canonical ensemble it can be demonstrated by numerical calculations. Integrability breaking perturbation (IBP) strongly reduces R which reveals a pronounced minimum at the crossover from anomalous diffusive to normal dissipative transport. This minimum coincides with the onset of the universality of the random matrix theory. Results for various IBP suggest a discontinuous jump of the spin conductivity in the thermodynamic limit, and moreover that its value universally decreases when the strength of IBP decreases.

Introduction. The transport and other properties of integrable quantum lattice models, the prominent example being the one-dimensional, anisotropic Heisenberg XXZ spin-1/2 chain, have in last decades reached higher level of understanding (for recent review see e.g. [1]) through the extended concepts of local [2] and quasilocal conserved quantities (CQ) [3, 4], via the analytical results emerging from the generalized hydrodynamics (GHD) [5–9] and with the application of various powerful numerical methods [10–15]. While the standard argument is that mastering of integrable models will be the crucial step to the proper description of closely related perturbed models, the advance in this direction is so far modest. In the case of the Heisenberg-type spin chains it appears evident that the integrability-breaking perturbations (IBP) suppress the finite-temperature ballistic transport, characterized by the spin stiffness $D(T > 0) > 0$, turning it into the normal dissipative one [16–20]. Still, analytical approaches and tools dealing with such perturbed systems are so far quite restricted [21–23].

The anisotropic Heisenberg chain in the easy-axis ($\Delta > 1$) regime represents a quite different challenge, with vanishing spin conductivity (and diffusion) at temperature $T \rightarrow 0$, as well as vanishing stiffness $D(T > 0) = 0$, but revealing finite spin diffusion constant \mathcal{D} even at high T [11, 13, 24, 25]. The diffusion is still anomalous in origin [26–28], and the transport is dissipationless [15]. Taking into account open questions in this problem, the introduction of IBP leads to even wider range of scenarios. While there appears general consensus that in large enough systems (system size $L \rightarrow \infty$) the spin transport becomes normal (i.e. dissipative), its variation with IBP strength g remains controversial. While some recent results indicate on the continuous variation of \mathcal{D} with g [29], there is also evidence for its discontinuity at $g \rightarrow 0$ [15, 30]. Moreover, introducing in the system a field $F > 0$ [12] even favors the vanishing of the spin conductivity with the vanishing $F \rightarrow 0$.

In this Letter we use an alternative approach to the

spin transport both in integrable and perturbed XXZ chains at $\Delta > 1$. Since these spin chains are equivalent to the models of interacting fermions, one can introduce a nonzero flux [31] that probes also system's response to changing of the boundary conditions. In particular, we employ the Thouless level sensitivity R . It was originally introduced into single-particle models to distinguish between conductors with $R \gg 1$ and insulators (localized systems) with $R \rightarrow 0$ [32] and has recently been applied also to interacting disordered systems [33].

The level sensitivity distinguishes also between ballistic and normal diffusive transport. In the former case it grows (up to logarithmic corrections) as the inverse of the mean level spacing, $R \propto 1/\Delta\epsilon$ whereas in generic diffusive systems this dependence is much weaker, namely $R \propto 1/\sqrt{\Delta\epsilon}$. We show that the diffusive transport in the easy-axis integrable XXZ chain ($\Delta > 1$) is anomalous in this respect. Namely, diffusive integrable chains reveal $R \propto 1/\Delta\epsilon$ in the grandcanonical ensemble (GCE), as well as in the canonical ensemble (CE) at total $S_{tot}^z = 0$. Therefore, the level sensitivity of diffusive integrable system differs from R in the ballistic systems only by logarithmic corrections, $\log(\Delta\epsilon)$, and is much larger than in generic diffusive models.

Large values of the level sensitivity in GCE, $R_{\text{GCE}} \gg 1$, can be explained by finding its strict lower bound through the overlap with the product of simplest integrals of motion of the XXZ model. On the other hand, level sensitivity obtained in CE, R_{CE} , strongly decreases with Δ . In a particular limit $\Delta \rightarrow \infty$, representing the 'folded' XXZ model [30, 34, 35], we even find strictly $R_{\text{CE}} = 0$. This result strongly contrasts with R_{GCE} for which the lower bound increases with Δ .

We also observe that R_{CE} in finite systems exhibits a nonmonotonic dependence on the strength of IBP, g . The minimum at $g = g^*(L)$ coincides with the crossover where the finite-size system starts to comply with the random matrix theory (RMT) [36, 37]. Therefore, the minimum of R allows us to delimit two regimes: $g > g^*(L)$ when

the system behaves as normal dissipative and $g < g^*(L)$ when the system properties are still dominated by finite-size effects. The meaning of the crossover can be confirmed also with standard indicators of RMT. Moreover, taking into account the restriction $g > g^*(L)$, one can then follow in a controlled way the variation with g of the d.c. spin conductivity in CE, σ_{CE} . Our results for two different classes of IBP seem to support a universal limit, i.e., vanishing of $\sigma_{\text{CE}}(g \rightarrow 0)$ in the thermodynamic limit.

XXZ Model with flux. We consider the XXZ spin ($s = 1/2$) chain of length L with periodic boundary conditions (PBC), introducing also the effect of finite flux, φ , into the exchange term

$$H = J \sum_l \left[\frac{1}{2} (e^{i\varphi} S_{l+1}^+ S_l^- + \text{H.c.}) + \Delta S_{l+1}^z S_l^z \right] + gH'. \quad (1)$$

We consider the easy-axis regime with the anisotropy $\Delta > 1$ and set $J = 1$ as the unit of energy. The spin model can be mapped on the model of interacting spinless fermions, where φL represents a magnetic flux through the ring [15, 31, 32]. We analyze two different prototype forms of IBP. In the main text, we discuss the next-nearest neighbor (nnn) interaction with $g = \Delta_2$ and $H' = \sum_l S_{l+2}^z S_l^z$, whereas in the Supplement [38] we study also the nnn exchange with $g = J_2$ and $H' = \sum_l [e^{2i\varphi} S_{l+1}^+ S_l^- S_{l-1}^- + \text{H.c.}]$ which maps to a nnn hopping in the fermionic chain.

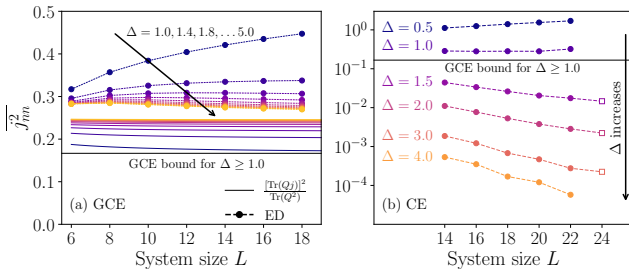


Figure 1. (a) GCE: bound from Eq. (5) (lines), compared with ED results (points) for the diagonal matrix elements, $\overline{j_{nn}^2}$. (b) CE: $\overline{j_{nn}^2}$ obtained via ED for the $S_{tot}^z = 0$ and various $\Delta = 0.5 - 4$. The horizontal line is the GCE bound, Eq. (5), that holds for $\Delta \geq 1$ and any L .

Level sensitivity and spin transport. The gauge transformation $S_l^\pm \rightarrow e^{\mp i\varphi} S_l^\pm$, $S_l^z \rightarrow S_l^z$ applied to the Hamiltonian (1) eliminates the flux dependence on all sites except the boundary term that takes the form $J/2(S_1^+ S_L^- e^{i\varphi L} + \text{H.c.})$. Then, the energy spectra, $H|n\rangle = \epsilon_n(\varphi)|n\rangle$, obtained for $\varphi = 0$ and $\varphi = \delta\varphi = \pi/L$ correspond, respectively, to periodic and antiperiodic ($J \rightarrow -J$) boundary conditions. Consequently, the level sensitivity to the boundary conditions is related to the derivative $\epsilon'_n(\varphi)$ that can be further simplified using an

identity for the spin-current operator, $j = dH/d\varphi$. Following the reasoning from Refs. [31, 39] one finds

$$\epsilon'_n(\varphi) = \frac{d}{d\varphi} \langle n|H|n\rangle = \langle n|j|n\rangle + \epsilon_n \frac{d}{d\varphi} \langle n|n\rangle = \langle n|j|n\rangle. \quad (2)$$

The level sensitivity introduced by Thouless in Ref. [32] is determined by the matrix elements of the spin-current operator, $j_{mn} = \langle n|j|m\rangle$,

$$R = \delta\varphi \sqrt{\overline{(\epsilon'_n(\varphi))^2}} / \Delta\epsilon = \delta\varphi \sqrt{\overline{j_{nn}^2}} / \Delta\epsilon, \quad \delta\varphi = \frac{\pi}{L}. \quad (3)$$

Here, overline means averaging over the eigenstates (in the relevant part of the spectrum) and $\Delta\epsilon$ is the average level spacing. We note that integrable XXZ model in the easy-plane regime $\Delta < 1$ exhibits a ballistic transport. It is quantified by the spin stiffness (Drude weight) [2], $D = \overline{j_{nn}^2} / L > 0$ that is finite in the thermodynamics limit $L \rightarrow \infty$. Consequently, in ballistic models one obtains $R = \pi\sqrt{D}/(\sqrt{L}\Delta\epsilon)$.

In the case of the easy-axis regime, $\Delta > 1$, the ballistic component vanishes in GCE and in CE with $S_{tot}^z = 0$. In both cases one finds $D = 0$ for $L \rightarrow \infty$. However in the GCE, one may still find a simple bound on the level sensitivity. To this end we employ the Mazur bound [2, 40], $\overline{j_{nn}^2} \geq [\text{Tr}(Qj)]^2 / \text{Tr}(Q^2)$ where Q is a conserved operator. We choose Q as a product of two simplest local conserved operators, $Q = Q_1 Q_3$, where $Q_1 = \sum_l S_l^z$ is the total magnetization and Q_3 is the energy current,

$$Q_3 = \frac{iJ}{2} \sum_l (JS_{l+1}^- S_l^z S_{l-1}^+ + \Delta S_{l+1}^z S_l^+ S_{l-1}^- + \Delta S_{l+1}^+ S_l^- S_{l-1}^z + \text{H.c.}). \quad (4)$$

Direct calculations in GCE give a bound

$$\overline{j_{nn}^2} \geq \frac{[\text{Tr}(Q_1 Q_3 j)]^2}{\text{Tr}(Q_1^2 Q_3^2)} = \frac{J^2 \Delta^2 L}{2J^2(L-2) + 4L\Delta^2}, \quad (5)$$

We present in Fig. 1(a) the GCE bound for different $\Delta \geq 1$ and compare it with the numerically evaluated value $\overline{j_{nn}^2}$ obtained in GCE for systems with $L \leq 18$. One can notice, that the lower bound even quantitatively approaches the numerical value at $\Delta \gg 1$. In the easy-axis regime, $\Delta > 1$, that is of interest here, one finds from Eq. (5) $\overline{j_{nn}^2} \geq 1/6$ and $R \geq (0.4\pi)/(L\Delta\epsilon)$. In the GCE, the level sensitivity in ballistic and diffusive regimes of the integrable XXZ chains differ only by a factor $1/\sqrt{L} \sim \mathcal{O}[\log(\Delta\epsilon)]$.

The above bound is inapplicable in the CE with $S_{tot}^z = 0$ because $Q_1 = 0$. Fig. 1(b) shows finite-size results for $\overline{j_{nn}^2}$. Here and further on, they are obtained using exact diagonalization (ED). For $L \leq 22$, we carry out full diagonalization for sectors with the wavevectors $0 < q < \pi$ and use half of the states from the middle of the spectra. For the largest $L = 24$ we employ

the shift-invert ED and randomly sample over $N \sim 150$ eigenstates from the middle of the spectra, in each sector with $0 < q < \pi$ (see Supplement [38] for details).

One observes that j_{nn}^2 is well below the GCE bound and that the difference between GCE and CE results increases with L and Δ . In order to elucidate such Δ -dependence, we have numerically studied also the 'folded' XXZ model [30, 34, 35] that represents $\Delta \rightarrow \infty$ limit of the XXZ chains, $H_f = (J/2) \sum_l P_l [e^{i\varphi} S_{l+1}^+ S_l^- + \text{H.c.}]$ with the projection operator $P_l = (S_{l+2}^z + S_{l-1}^z)^2$ that introduces conservation of the number of domain walls. In this model we find (so far numerically) strictly $j_{nn}^2 = 0$ for any L . Consequently, one gets $R_{CE} = 0$ while $R_{GCE} > 0$ as it follows from the strict bound in Eq. (5).

Following results in Fig. 1(b) we present in Fig. 2(a) the dependence of R_{CE} on the average level spacing $\Delta\epsilon$. Results show that for finite $\Delta < \infty$, the anomalous dependence $R \propto 1/\Delta\epsilon$ holds true up to logarithmic corrections, $\mathcal{O}[\log(\Delta\epsilon)]$, being thus close to ballistic systems rather than to generic diffusive ones, as discussed further on.

The properties of R in chaotic models are related to the d.c. spin conductivity $\tilde{\sigma}$ via the RMT relations [41–43]. Since at high $T \gg J$ one gets $\tilde{\sigma} \propto T^{-1}$, we consider here a rescaled $\sigma = T\tilde{\sigma}$, defined as the (Kubo) linear-response function

$$\sigma = \lim_{\omega \rightarrow 0} \frac{\pi}{LN_{st}} \sum_{n \neq m} |j_{mn}|^2 \delta(\omega - \epsilon_m + \epsilon_n) \simeq \frac{\pi \overline{|j_{mn}|^2}}{L\Delta\epsilon}, \quad (6)$$

where N_{st} is the Hilbert-space dimension, and $\overline{|j_{mn}|^2}$ are averaged matrix elements for small $|\epsilon_m - \epsilon_n|$. Upon introducing a flux $\varphi \neq 0$, the degeneracy of energy levels persists only in momentum sectors $q = 0$ and $q = \pi$. All other sectors obey the RMT relations [43], which in our system follow the Gaussian orthogonal ensemble (GOE) universality, requiring $Y = \overline{|j_{mn}|^2}/\overline{j_{nn}^2} = 1/2$. Therefore, RMT establishes a link between the level sensitivity, Eq. (3) and the spin conductivity, Eq. (6),

$$R = \sqrt{\frac{2\pi\sigma}{L\Delta\epsilon}}. \quad (7)$$

Consequently, introducing of IBP must be accompanied by a substantial drop of the level sensitivity from $R \propto 1/(L\Delta\epsilon)$ in the integrable chain (either ballistic or diffusive) to $R \propto 1/\sqrt{L\Delta\epsilon}$ in the chaotic system. In the GCE, such scenario is a direct consequence of the bound in Eq. (5). In the CE with finite $\Delta < \infty$ we confirm this scenario via numerical calculations and all result henceforth apply to the latter.

Fig. 2(a) confirms that substantial IBP ($g = \Delta_2$) causes qualitative changes of R_{CE} , as discussed in the preceding paragraphs. More systematic dependence of R_{CE} on the IBP strength Δ_2 is presented in Figs. 2(b)-2(d) for different $\Delta > 1$. One observes that R_{CE} develops

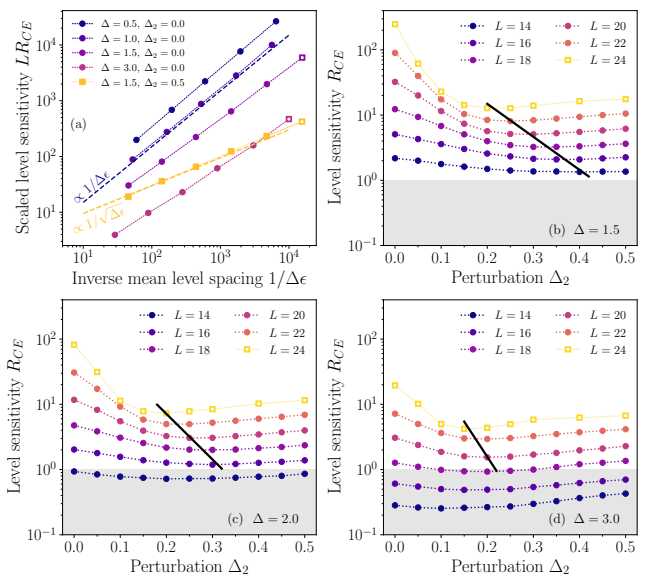


Figure 2. Results for CE with $S_{tot}^z = 0$ from full ED (filled symbols) and shift-invert method (open symbols). (a) Scaled level sensitivity LR_{CE} vs $1/\Delta\epsilon$, where $\Delta\epsilon$ is average level spacing in sectors with fixed momenta. Dashed lines are guidelines showing $1/\Delta\epsilon$ and $1/\sqrt{\Delta\epsilon}$ dependence, respectively. (b)-(d) R_{CE} vs. IBP strength Δ_2 for $\Delta = 1.5, 2.0, 3.0$. Thick black lines mark the minima of $R(\Delta_2)$ while regions with $R < 1$ are shaded.

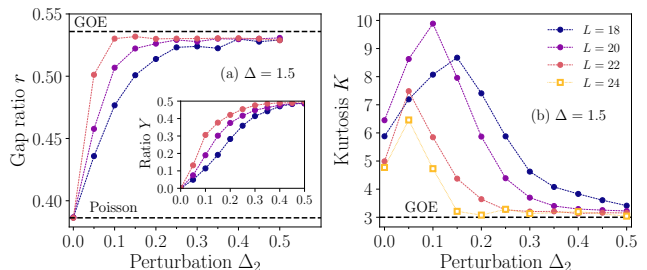


Figure 3. RMT indicators for the perturbed model in canonical sector. a) Gap ratio r , inset: ratio Y of off-diagonal and diagonal matrix elements. b) Kurtosis K (defined in text).

a clear minimum at finite Δ_2 that drifts towards weaker IBP when L increases. It should be noted, that we are interested in the regime $R_{CE} \gtrsim 1$. For $R_{CE} \lesssim 1$ (shaded areas in Fig. 2) the system is too small, i.e. the level spacing is too large, so that changing of the flux causes neither level crossings nor avoided crossings (within the same S_{tot}^z and momentum sector).

In order to explain the origin of this minimum, we numerically study the standard indicators of RMT. The main panel in Fig. 3(a) shows the gap ratio $r = \bar{r}_n$ with $r_n = \min[\Delta_n, \Delta_{n+1}]/\max[\Delta_n, \Delta_{n+1}]$, where $\Delta_n = \epsilon_{n+1} - \epsilon_n$. The inset shows the ratio of the off-diagonal and the diagonal matrix elements, $Y = \overline{|j_{mn}|^2}/\overline{|j_{nn}|^2}$. Both results confirm that sufficiently

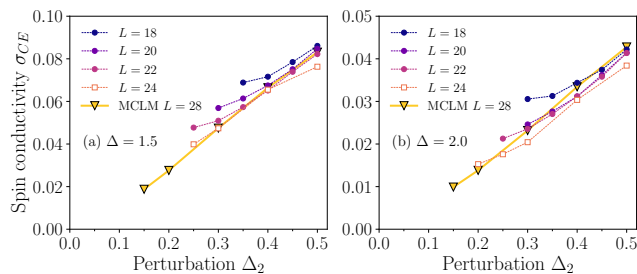


Figure 4. Spin conductivity in canonical sector, σ_{CE} , for: (a) $\Delta = 1.5$ and (b) $\Delta = 2.0$. Results obtained from diagonal matrix elements via full ED ($L = 18 - 22$) and shift-invert ($L = 24$) are presented in the regime $\Delta_2 > \Delta_2^*(L)$, i.e., above the crossover to the GOE universality. Presented are also MCLM results for $L = 28$.

strong IBP introduces the GOE universality [44, 45] with $Y = 0.5$ and $r \simeq 0.53$. Fig. 3(b) shows the kurtosis $K = \overline{j_{nn}^4} / \left(\overline{j_{nn}^2}\right)^2$. At large enough Δ_2 , K agrees with the kurtosis of the Gaussian distribution with $K = 3$. Comparing results in Figs. 2 and 3 one finds that minimum in R_{CE} corresponds to the crossover to the normal RMT behavior. In other words, the minimum reveals the threshold strength of IBP, $g^*(L)$, when the scattering becomes strong enough to introduce the RMT universality.

In systems which satisfy RMT, the spin conductivity, σ , can be obtained also from the diagonal matrix elements, $\overline{|j_{nn}|^2}$, via Eqs. (3) and (7). Fig. 4 shows such results for the spin conductivity in CE, σ_{CE} . As before we use $g = \Delta_2$ as IBP. In Fig. 4 we present only numerical results which are beyond the crossover to the GOE universality, i.e. obtained for $g > g^*(L)$. The minima in R_{CE} in Figs. 2(b)- 2(d) are here visible as the starting points of curves for various L . In Fig. 4 we show also results obtained from the microcanonical Lanczos method (MCLM) [46, 47]. This method allows to evaluate full dynamical $\sigma_{CE}(\omega)$, and consequently also σ_{CE} as in Eq. (6), for larger systems, but with smaller frequency resolution $\delta\omega$. Here, we present MCLM results for $L = 28$ with $\delta\omega \lesssim 10^{-3}$ [15], which we estimate to be meaningful at least down to $g = \Delta_2 \sim 0.15$.

We note that results for σ_{CE} obtained from various methods are consistent provided that $g > g^*(L)$. One also observes that σ_{CE} strongly depends on Δ resembling the analogous dependence of R_{CE} on Δ shown Fig. 2(a). Apparently for $g > g^*(L)$, the spin conductivity follows the relation $\sigma_{CE} \propto |g|$. Here we can make a link with the diffusion constant, \mathcal{D} . In generic dissipative system it is related to σ via the Einstein relation, that at large T reads $\mathcal{D} = 4\sigma$. The diffusion has been studied extensively in the integrable case and evaluated mostly in the GCE, both analytically within the GHD [25] and numerically via various methods [11, 13–15, 26] leading to values $\mathcal{D}_{GCE} > 0.4$ in the regime $\Delta > 1$. Evidently, σ_{CE} shown

in Fig. 4 for perturbation $g > g^*(L)$ is well below the latter. This discrepancy suggests a discontinuous change of \mathcal{D} upon the introduction of IBP in agreement with Refs. [15, 30]. Here, the underlying assumptions are the Einstein relation and the equivalence of CE and GCE. Numerical testing of the latter equivalence for weakly perturbed systems is extremely demanding since the difference between both ensembles approximately follows the relation $\mathcal{D}_{GCE} - \mathcal{D}_{CE} \propto 1/(g^2 L)$ [15].

The relevant question is how general are conclusions presented above for a particular form of IBP with $g = \Delta_2$. In the Supplemental Material [38] we therefore present analogous results for another class of IBP, i.e. for $g = J_2$ representing the nnn exchange. Conclusions are quite similar to the above ones for $g = \Delta_2$, even that concerning the apparent vanishing $\sigma_{CE}(g \rightarrow 0) \rightarrow 0$. The difference is that $J_2 > 0$ introduces nonvanishing matrix elements $\overline{|j_{nn}|^2} > 0$ also in the folded model.

Conclusions and Discussion We have studied sensitivity of the energy levels to the flux (or equivalently twisted boundary conditions), R , and related transport quantities, within the XXZ chain in the easy-axis regime. Although the transport in the integrable model is diffusive, obtained R is very close to one in integrable ballistic systems and, up to logarithmic corrections, exhibits the same dependence on the level spacing, $R \propto 1/\Delta\epsilon$. It strongly contrasts with chaotic diffusive systems where $R \propto 1/\sqrt{\Delta\epsilon}$. In the case of GCE, we have found for integrable chain a strict bound $R_{GCE} \geq 0.4\pi/(L\Delta\epsilon)$ that holds for arbitrary anisotropy $\Delta \geq 1$ and all system sizes, L . In the CE and for finite anisotropy $\Delta < \infty$, the level sensitivity still varies as $R_{CE} \propto 1/\Delta\epsilon$, however R_{CE} is much smaller than R_{GCE} . The difference between R_{GCE} and R_{CE} grows with the systems sizes and anisotropy. In the limiting case $\Delta \rightarrow \infty$ we have found that R_{CE} strictly vanishes for all system sizes whereas R_{GCE} is bounded from below.

The qualitative difference between the level sensitivity in integrable and chaotic systems implies that a perturbation of strength g must cause a substantial reduction of R . In finite systems, R_{CE} is minimal at the crossover between integrable and RMT regimes. The minimum at $g = g^*(L)$ shifts towards weaker perturbations with increasing L .

In the chaotic regime, RMT establishes the Thouless-like relation between R and the d.c. spin conductivity, σ . Using this relation we have numerically studied σ in CE and found for $g > g^*(L)$ that $\sigma_{CE} \propto |g|$. For weak perturbations, σ_{CE} becomes much smaller than σ_{GCE} estimated from the diffusion constant for integrable systems. Assuming that the Einstein relation and the equivalence between CE and GCE hold true for all model parameters, our results support a discontinuous variation of $\sigma_{GCE} = \sigma_{CE}$ with IBP. It should be acknowledged that the limit of a weak perturbation is highly nontrivial since the difference between CE and GCE results goes as,

$1/(g^2L)$ [15]. Consequently, the convergence of results in both ensembles would be hard to establish numerically.

Acknowledgments. We acknowledge fruitful discussions with L. Zadnik and R. Steinigeweg. M.M. acknowledges support by the National Science Centre (NCN), Poland via project 2020/37/B/ST3/00020. J.P. acknowledges support by the National Science Centre (NCN), Poland via project 2023/49/N/ST3/01033. P. P. acknowledges support of the Slovenian Research Agency via the program P1-0044.

-
- [1] B. Bertini, F. Heidrich-Meisner, C. Karrasch, T. Prosen, R. Steinigeweg, and M. Žnidarič, Finite-temperature transport in one-dimensional quantum lattice models, *Rev. Mod. Phys.* **93**, 025003 (2021).
- [2] X. Zotos, F. Naef, and P. Prelovšek, Transport and conservation laws, *Phys. Rev. B* **55**, 11029 (1997).
- [3] T. Prosen, Open XXZ spin chain: Nonequilibrium steady state and a strict bound on ballistic transport, *Phys. Rev. Lett.* **106**, 217206 (2011).
- [4] T. Prosen and E. Ilievski, Families of quasilocal conservation laws and quantum spin transport, *Phys. Rev. Lett.* **111**, 057203 (2013).
- [5] B. Bertini, M. Collura, J. De Nardis, and M. Fagotti, Transport in out-of-equilibrium XXZ chains: Exact profiles of charges and currents, *Phys. Rev. Lett.* **117**, 207201 (2016).
- [6] O. A. Castro-Alvaredo, B. Doyon, and T. Yoshimura, Emergent hydrodynamics in integrable quantum systems out of equilibrium, *Phys. Rev. X* **6**, 041065 (2016).
- [7] E. Ilievski and J. De Nardis, Microscopic Origin of Ideal Conductivity in Integrable Quantum Models, *Phys. Rev. Lett.* **119**, 020602 (2017).
- [8] V. B. Bulchandani, R. Vasseur, C. Karrasch, and J. E. Moore, Bethe-Boltzmann hydrodynamics and spin transport in the XXZ chain, *Phys. Rev. B* **97**, 045407 (2018).
- [9] J. De Nardis, D. Bernard, and B. Doyon, Hydrodynamic diffusion in integrable systems, *Phys. Rev. Lett.* **121**, 160603 (2018).
- [10] X. Zotos and P. Prelovšek, Evidence for ideal insulating or conducting state in a one-dimensional integrable system., *Phys. Rev. B* **53**, 983 (1996).
- [11] M. Žnidarič, Spin transport in a one-dimensional anisotropic Heisenberg model, *Phys. Rev. Lett.* **106**, 220601 (2011).
- [12] M. Mierzejewski, J. Bonča, and P. Prelovšek, Integrable mott insulators driven by a finite electric field, *Phys. Rev. Lett.* **107**, 126601 (2011).
- [13] C. Karrasch, J. E. Moore, and F. Heidrich-Meisner, Real-time and real-space spin and energy dynamics in one-dimensional spin-1/2 systems induced by local quantum quenches at finite temperatures, *Phys. Rev. B* **89**, 075139 (2014).
- [14] R. Steinigeweg, J. Gemmer, and W. Brenig, Spin and energy currents in integrable and nonintegrable spin-1/2 chains: A typicality approach to real-time autocorrelations, *Phys. Rev. B* **91**, 104404 (2015).
- [15] P. Prelovšek, S. Nandy, Z. Lenarčič, M. Mierzejewski, and J. Herbrych, From dissipationless to normal diffusion in the easy-axis heisenberg spin chain, *Phys. Rev. B* **106**, 245104 (2022).
- [16] H. Castella and X. Zotos, Finite-temperature mobility of a particle coupled to a fermionic environment, *Phys. Rev. B* **54**, 4375 (1996).
- [17] P. Jung, R. W. Helmes, and A. Rosch, Transport in almost integrable models: Perturbed Heisenberg chains, *Phys. Rev. Lett.* **96**, 067202 (2006).
- [18] P. Jung and A. Rosch, Spin conductivity in almost integrable spin chains, *Phys. Rev. B* **76**, 245108 (2007).
- [19] M. Žnidarič, Weak integrability breaking: Chaos with integrability signature in coherent diffusion, *Phys. Rev. Lett.* **125**, 180605 (2020).
- [20] M. Mierzejewski, J. Pawłowski, P. Prelovšek, and J. Herbrych, Multiple relaxation times in perturbed XXZ chain, *SciPost Phys.* **13**, 013 (2022).
- [21] A. J. Friedman, S. Gopalakrishnan, and R. Vasseur, Diffusive hydrodynamics from integrability breaking, *Phys. Rev. B* **101**, 180302 (2020).
- [22] A. Bastianello, A. D. Luca, and R. Vasseur, Hydrodynamics of weak integrability breaking, *J. Stat. Mech.* **2021**, 114003 (2021).
- [23] J. De Nardis, S. Gopalakrishnan, R. Vasseur, and B. Ware, Stability of superdiffusion in nearly integrable spin chains, *Phys. Rev. Lett.* **127**, 057201 (2021).
- [24] R. Steinigeweg, J. Herbrych, P. Prelovšek, and M. Mierzejewski, Coexistence of anomalous and normal diffusion in integrable mott insulators, *Phys. Rev. B* **85**, 214409 (2012).
- [25] S. Gopalakrishnan and R. Vasseur, Kinetic theory of spin diffusion and superdiffusion in XXZ spin chains, *Phys. Rev. Lett.* **122**, 127202 (2019).
- [26] P. Prelovšek, S. E. Shawish, X. Zotos, and M. Long, Anomalous scaling of conductivity in integrable fermion systems, *Phys. Rev. B* **70**, 205129 (2004).
- [27] M. Žnidarič, Anomalous nonequilibrium current fluctuations in the heisenberg model, *Phys. Rev. B* **90**, 115156 (2014).
- [28] M. Medenjak, C. Karrasch, and T. Prosen, Lower bounding diffusion constant by the curvature of drude weight, *Phys. Rev. Lett.* **119**, 080602 (2017).
- [29] M. Kraft, M. Kempa, J. Wang, S. Nandy, and R. Steinigeweg, Scaling of diffusion constants in perturbed easy-axis Heisenberg spin chains (2024), [arXiv:2410.22586](https://arxiv.org/abs/2410.22586).
- [30] J. De Nardis, S. Gopalakrishnan, R. Vasseur, and B. Ware, Subdiffusive hydrodynamics of nearly-integrable anisotropic spin chains, *PNAS* **119**, e2202823119 (2022).
- [31] W. Kohn, Theory of the insulating state, *Phys. Rev.* **133**, A171 (1964).
- [32] J. T. Edwards and D. J. Thouless, Numerical studies of localization in disordered systems, *Journal of Physics C: Solid State Physics* **5**, 807 (1972).
- [33] P. Prelovšek, J. Herbrych, and M. Mierzejewski, Slow diffusion and Thouless localization criterion in modulated spin chains, *Phys. Rev. B* **108**, 035106 (2023).
- [34] L. Zadnik and M. Fagotti, The Folded Spin-1 / 2 XXZ Model : I. Diagonalization, Jamming, and Ground State Properties, *SciPost Phys. Core* **4**, 010 (2021).
- [35] L. Zadnik, K. Bidzhev, and M. Fagotti, The folded spin-

- 1=2 XXZ model: II. Thermodynamics and hydrodynamics with a minimal set of charges, *SciPost Physics* **10**, 1 (2021).
- [36] T. A. Brody, J. Flores, J. B. French, P. A. Mello, A. Pandey, and S. S. M. Wong, Random-matrix physics: spectrum and strength fluctuations, *Rev. Mod. Phys.* **53**, 385 (1981).
- [37] M. Wilkinson, Diffusion and dissipation in complex quantum systems, *Phys. Rev. A* **41**, 4645 (1990).
- [38] See Supplemental Material for details on shift-invert method and additional results with next-nearest-neighbor exchange as the perturbation.
- [39] H. Castella, X. Zotos, and P. Prelovšek, Integrability and ideal conductance at finite temperatures, *Phys. Rev. Lett.* **74**, 972 (1995).
- [40] P. Mazur, Non-ergodicity of phase functions in certain systems, *Physica* **43**, 533 (1969).
- [41] J. M. Deutsch, Quantum statistical mechanics in a closed system, *Phys. Rev. A* **43**, 2046 (1991).
- [42] M. Srednicki, The approach to thermal equilibrium in quantized chaotic systems, *Journal of Physics A: Mathematical and General* **32**, 1163 (1999).
- [43] L. D'Alessio, Y. Kafri, A. Polkovnikov, and M. Rigol, From quantum chaos and eigenstate thermalization to statistical mechanics and thermodynamics, *Advances in Physics* **65**, 239 (2016).
- [44] V. Oganesyan and D. A. Huse, Localization of interacting fermions at high temperature, *Physical Review B* **75**, 155111 (2007).
- [45] Y. Y. Atas, E. Bogomolny, O. Giraud, and G. Roux, Distribution of the ratio of consecutive level spacings in random matrix ensembles, *Physical Review Letters* **110**, 1 (2013).
- [46] M. W. Long, P. Prelovšek, S. El Shawish, J. Karadamoglou, and X. Zotos, Finite-temperature dynamical correlations using the microcanonical ensemble and the lanczos algorithm, *Phys. Rev. B* **68**, 235106 (2003).
- [47] P. Prelovšek and J. Bonča, Ground state and finite temperature lanczos methods, in *Strongly Correlated Systems - Numerical Methods*, edited by A. Avella and F. Mancini (Springer, Berlin, 2013).
- [48] F. Pietracaprina, N. Macé, D. J. Luitz, and F. Alet, Shift-invert diagonalization of large many-body localizing spin chains, *SciPost Physics* **5**, 10.21468/scipostphys.5.5.045 (2018).

Supplemental Material: Transport in integrable and perturbed easy-axis Heisenberg chain: Thouless approach.

J. Pawłowski¹, M. Mierzejewski¹, and P. Prelovšek²

¹ *Institute of Theoretical Physics, Faculty of Fundamental Problems of Technology, Wrocław University of Science and Technology, 50-370 Wrocław, Poland*

² *J. Stefan Institute, SI-1000 Ljubljana, Slovenia*

In the Supplemental Material we present additional results with next-nearest-neighbor exchange as the perturbation and details about shift-invert calculations.

Next-nearest-neighbor exchange as the perturbation: results

In addition to the next-nearest-neighbor (nnn) interaction $g = \Delta_2$ taken as the integrability-breaking perturbation (IBP) we present analogous results also for the nnn exchange where $g = J_2$ and

$$H' = \sum_l [e^{2i\varphi} S_{l+1}^+ S_l^z S_{l-1}^- + \text{H.c.}]. \quad (\text{S1})$$

We note that such term maps to a nnn hopping in the fermionic chain.

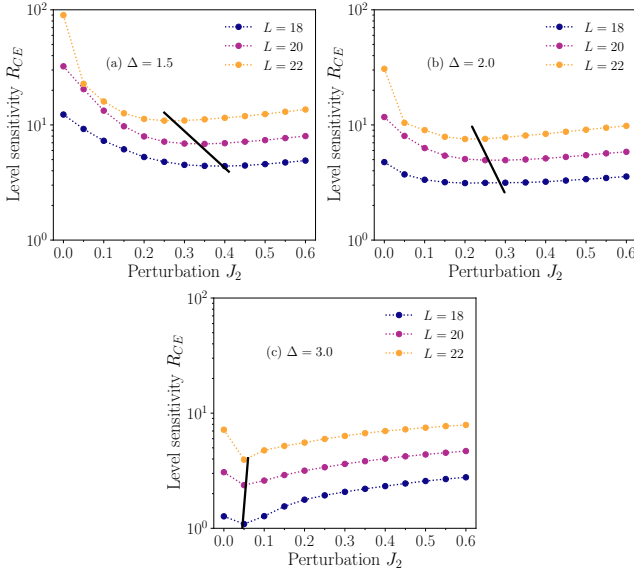


Figure S1. Level sensitivity R_{CE} vs. perturbation strength J_2 within sector $S_{tot}^z = 0$, as calculated via full ED in systems with $L = 18 - 22$ sites, for: (a) $\Delta = 1.5$, (b) $\Delta = 2.0$, and (c) $\Delta = 3.0$.

We first present in Fig. S1 results for the level sensitivity R varying the IBP strength J_2 , as calculated via full ED in systems with $L = 18 - 22$. Again, substantial IBP ($J_2 \gg 0$) causes qualitative changes of R , inducing a minimum of $R(J_2)$ indicating the crossover into the regime $J_2 > J_2^*(L)$ with RMT universality. As in the main text, also here we restrict to the regime $R > 1$ where the interpretation of results in terms of normal transport is

meaningful. While the behavior is quite similar to the case of $g = \Delta_2$, presented in the main text, it should be noticed that the dependence of R on Δ in Fig. S1 is less pronounced than for Δ_2 . Larger values of R in the present case allow us also to reach $R > 1$ also for $\Delta = 3$. The qualitative difference emerges at $\Delta \rightarrow \infty$ where in the folded model with $\Delta_2 \neq 0$ one obtains $R = 0$, while this is not the case for $g = J_2$ which introduced $R > 0$ even in the folded model.

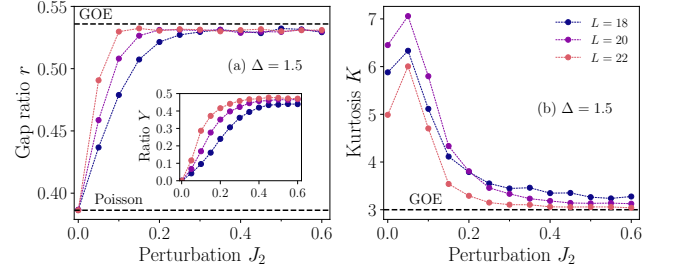


Figure S2. RMT indicators for the model with J_2 perturbation. a) Gap ratio r , inset: ratio Y of off-diagonal matrix elements versus the diagonal ones. b) Kurtosis K (defined in the text).

We present in Fig. S2 results for standard indicators of RMT: in Fig. S2(a) the gap ratio $r = \bar{r}_n$ with $r_n = \min[\Delta_n, \Delta_{n+1}] / \max[\Delta_n, \Delta_{n+1}]$, in the inset of Fig. S2(a) the ratio $Y = |j_{mn}|^2 / |j_{nn}|^2$, and finally in Fig. S2(b) the kurtosis $K = \bar{j}_{nn}^4 / (\bar{j}_{nn}^2)^2$. All results again confirm that sufficiently strong IBP $g > g^*(L)$ introduces the GOE universality with $Y = 0.5$, $r \simeq 0.53$, and $K \simeq 3$.

Finally, we show results for σ_{CE} beyond the crossover to the GOE universality $g > g^*(L)$ for $g = J_2$, here obtained via ED with up to $L = 22$. Again, results for σ_{CE} become quantitatively consistent (weakly L -dependent) provided that $g > g^*(L)$. Extrapolating the crossover $g^*(L)$ to larger L , we can compare then results to those obtained via MCLM for larger $L = 24$ and $L = 28$, which then apparently leads to RMT-meaningful results down to $g = J_2 \sim 0.2$ as presented in Fig. S3. The conclusion are analogous to one presented for $g = \Delta_2$. The difference again is that the dependence of σ_{CE} on Δ for $g = J_2$ is weaker than for $g = \Delta_2$. Namely, σ_{CE} at $J_2 > 0$ remains

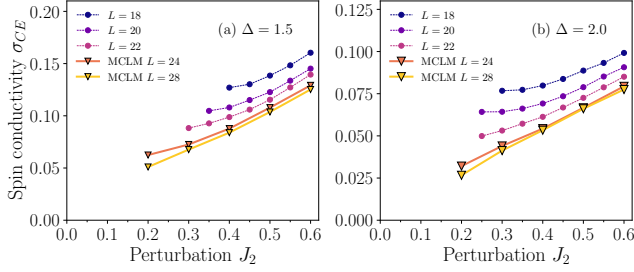


Figure S3. Spin conductivity σ_{CE} for (a) $\Delta = 1.5$ and (b) $\Delta = 2.0$. Points denote results obtained from diagonal matrix elements via full ED ($L = 18 - 22$), presented in the regime $J_2 > J_2^*(L)$, i.e., above the crossover to the GOE universality. Presented are also MCLM results for $L = 24$ and $L = 28$.

substantial also in the limit $\Delta \rightarrow \infty$, i.e., within the folded model. Otherwise, for $J_2 \ll 0.5$ the values of σ_{CE} are well below the integrable GCE value $\sigma_{GCE} > 0.1$ indicating on the discontinuous jump at $g \rightarrow 0$. Moreover, the variation of σ_{CE} with g in Fig. S3 reveals $\sigma_{CE} \propto |g|$ for $g > g^*(L)$. However, as in the main text we stress that the regime of weak IBP should be taken with care and requires further attention.

Numerical methods

We evaluate the diagonal matrix elements of the spin current for $L = 24$ using a custom implementation of the shift-invert method [48], employing Intel oneMKL for matrix-vector multiplication and oneMKL PARDISO linear solver to compute the action of $(H - E)^{-1}$ on vectors. The essence of this approach is to apply the standard Lanczos algorithm to the resolvent $(H - E)^{-1}$, where E is a target energy, in our case selected randomly from the middle half of the spectrum. Using the resolvent of the

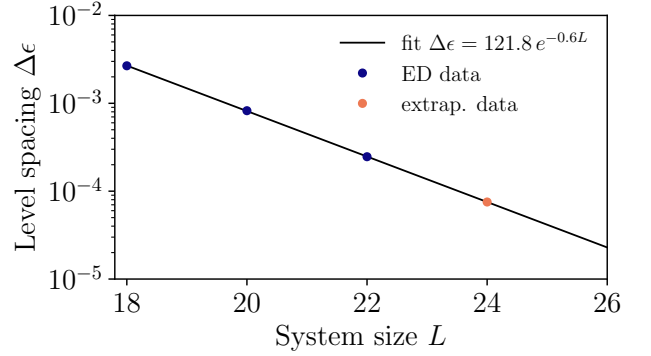


Figure S4. Mean level spacing $\Delta\epsilon$ vs. system size L for $\Delta = 2.0$ and $\Delta_2 = 0.1$. Dark blue points correspond to ED data for $L = 18, 20, 22$ and orange point to the extrapolated value for $L = 24$, used in subsequent shift-invert calculations.

Hamiltonian turns a dense part of the spectrum into a sparse one, facilitating the convergence of Lanczos procedure. In this way, we can sample the relevant eigenstates and approximate moments of j_{nn} without performing a full diagonalization. We find $M = 30$ Lanczos steps and 100 – 150 states per momentum sector being enough for the results to converge. However, there is some caution required, as the action of the resolvent on a vector results in a system of linear equations $(H - E)|w\rangle = |v\rangle$, that is severely ill-conditioned, with condition number $\kappa \propto \exp L$. Hence, iterative solvers usually fail to reach satisfying precision, and direct solvers have to be used instead, limiting accessible systems sizes.

To compute the level sensitivity R and spin conductivity σ_{CE} (Eq. (3) and Eq. (6) in the main text), we also require the mean level spacing $\Delta\epsilon$ in the central part of the spectrum. Taking into account the exponential dependence of $\Delta\epsilon$ on the size of the system, it is straightforward to extrapolate this value from the ED data for $L = 18, 20, 22$. An example of such an extrapolation for the case of $\Delta = 2.0$ and $\Delta_2 = 0.1$ is shown in Fig. S4.